*J. Fluid Mech.* (1983), *vol.* 135, *pp.* 51–69
*Printed in Great Britain*



# Sliding sheets: lubrication with comparable viscous and inertia forces

By E. O. TUCK
Applied Mathematics Department, University of Adelaide
AND M. BENTWICH
Department of Fluid Mechanics and Heat Transfer, Tel Aviv University

(Received 19 October 1982 and in revised form 1 June 1983)

A rigid plane thin sheet is sliding steadily at speed $U$ close to a plane wall, in a fluid of kinematic viscosity $\nu$. The sheet is infinitely wide and is of length $L$ in the direction of motion, and its leading edge is a distance $h_0 \ll L$ from the wall. A solution is sought for arbitrary finite values of $R = Uh_0^2/\nu L$. In the limit as $\epsilon = h_0/L \to 0$, the problem reduces to that of solving the boundary-layer equation in the gap region between sheet and wall, and this is done here both by an empirical linearization, and by direct numerical methods. The solutions have the property that they reduce to those predicted by lubrication theory when $R$ is small, and to those predicted by an inviscid small-gap theory when $R$ is large. Special attention is paid to the correct entrance and exit conditions, and to the location of the centre of pressure.

## 1. Introduction

Consider two types of flow in a narrow gap. One is that described by the so-called 'lubrication theory' (e.g. as in Cameron 1966). In its simplest form, this theory assumes (in addition to narrowness of the gap), that inertia is negligible, and that the pressure vanishes at entrance and exit from the gap.

For example, let the upper boundary $y = h(x)$, $0 \leqslant x \leqslant L$, of a two-dimensional flow domain be fixed in space, while the lower plane boundary $y = 0$ moves at velocity $U$ past it, in an incompressible fluid of viscosity $\mu$. Then, according to lubrication theory, the pressure $p$ is a function of $x$ only, and the stream function $\psi(x, y)$ is a cubic function of $y$. Enforcing the boundary conditions at $y = 0$ and $y = h(x)$ leads immediately to Reynolds' equation for the pressure, whose solution with zero end pressures is

$$p(x) = 6\mu U \int_0^x \left[ h^{-2}(x) - \frac{\int_0^L h^{-2}(\xi)\,\mathrm{d}\xi}{\int_0^L h^{-3}(\xi)\,\mathrm{d}\xi} h^{-3}(x) \right] \mathrm{d}x. \tag{1.1}$$

In particular, for a flat plate at angle of attack $\alpha$, i.e.

$$h(x) = h_0 - \alpha x, \tag{1.2}$$

we have

$$p(x) = \frac{3\mu U \alpha}{h(\frac{1}{2}L)} \frac{x(L-x)}{(h(x))^2}. \tag{1.3}$$

On the other hand, if the boundary $y = h(x)$ is the lower surface of an airfoil in ground effect, then (Tuck, 1980, 1981) an almost-conventional aerodynamic analysis can be performed, to determine the net circulation and the pressure, providing we assume that the viscosity is negligible, and that the pressure vanishes at the trailing edge. The resulting 'inviscid small-gap theory' has the property that the velocity is predominantly in the $x$-direction and uniform with respect to $y$, and its magnitude is inversely proportional to $h(x)$. If we substitute this result into the Bernoulli equation, and enforce the trailing-edge condition, the result for the pressure is

$$p(x) = \tfrac{1}{2}\rho U^2\left[1 - \left(\frac{h(L)}{h(x)}\right)^2\right] \tag{1.4}$$

for all $h(x)$, where $\rho$ is the (constant) fluid density.

The results (1.3) and (1.4) have some features in common, and some of stark contrast. In both cases, the pressure depends on $x$ alone, and vanishes at $x = L$. But the assumptions from which these two results are obtained are incompatible with each other; indeed *opposite* in effect. The pressure (1.3) is proportional to the viscosity $\mu$ and independent of the density $\rho$; the reverse is true of (1.4), indicating the relative importance of viscosity and inertia in each case.

Another interesting point of difference between (1.3) and (1.4) concerns the actual $x$-wise variation in pressure. In neither case is the distribution symmetric about the midpoint $x = \frac{1}{2}L$. In lubrication theory, the greatest forces tend to occur in the narrowest gaps, so that the centre of pressure for (1.3) is toward the *rear*, with $x > \frac{1}{2}L$. On the other hand, the Bernoulli forces on a ground-effect airfoil are greatest where the velocity is least, and this is where the gap is at its widest, so that the centre of pressure for (1.4) is toward the leading edge, with $x < \frac{1}{2}L$.

This particular difference was noted by Tuck (1982) as a factor in free sliding of a uniform plane sheet over a plane surface. Equilibrium with respect to pitching rotations demands that the centre of pressure and centre of gravity coincide, and this cannot be the case for a flat rigid sheet, in *either* the lubrication mode (1.3) or aerodynamic mode (1.4). Tuck (1982) overcame this difficulty in the aerodynamic mode by allowing the sheet to bend.† However, in view of the opposite tendencies of the centre of pressure in the two modes, it is attractive to consider some kind of 'amalgam' of the two modes, in which it may be possible for the centre of pressure to be at the midpoint, even for a rigid sheet.

Clearly (1.3) and (1.4) represent opposite limiting extremes of any such more general theory. If we note that the order of magnitude of (1.3) is

$$p_{\mathrm{V}} = \mu UL/h_0^2 \tag{1.5}$$

while that of (1.4) is

$$p_{\mathrm{I}} = \rho U^2, \tag{1.6}$$

it is apparent that the general theory will have to encompass a range in which $p_{\mathrm{V}}$ and $p_{\mathrm{I}}$ are comparable in magnitude, i.e. in which

$$R = \frac{p_{\mathrm{I}}}{p_{\mathrm{V}}} = \frac{Uh_0^2}{\nu L} \tag{1.7}$$

is of unit order. Then (1.3) will be the limit as $R \to 0$ and (1.4) the limit as $R \to \infty$, of this theory.

† Bending does not help in the lubrication mode, since in that mode, if we allow the fluid pressure to bend the sheet, this moves the centre of pressure *further* toward the rear.

Just what kind of theory is needed? Clearly we can no longer assume that either inertia or viscosity is negligible. However, we must retain and use the common assumption that the gap is narrow relative to its length, so that

$$\epsilon = \frac{h_0}{L} \ll 1. \tag{1.8}$$

But such a theory has long existed; it is nothing more or less than Prandtl's boundary-layer theory! Indeed, it has already been recognized by workers on entrance flows in pipes and ducts (see e.g. Schlichting 1960, p. 169; Williams 1963; Sparrow, Lin & Lundgren 1964; Keller 1975) that the boundary-layer equation

$$\psi_y \psi_{xy} - \psi_x \psi_{yy} = -\frac{1}{\rho} p'(x) + \nu \psi_{yyy} \tag{1.9}$$

can be used to describe the *whole* flow in such a duct, not just the conventional boundary layers close to the walls.

The only difference between this 'internal' application of boundary-layer theory, and the original one of Prandtl for 'external' boundary layers, is that the pressure gradient $p'(x)$ is now *unknown*. The flow domain is bounded by a surface of *known* geometry $y = h(x)$, and we have 4 rather than 3 boundary conditions, namely

$$\psi = 0, \quad \psi_y = U \quad \text{on} \quad y = 0, \tag{1.10}$$

$$\psi_x = \psi_y = 0 \quad \text{on} \quad y = h(x). \tag{1.11}$$

Such problems have been termed 'inverse' boundary-layer problems by Keller (1978).

The fact that the boundary-layer equation (1.9) holds formally for $R = O(1)$, where $R$ is given by (1.7), is now apparent. Thus, in general, boundary layers grow in the $x$-direction, starting at $x = 0$, and have thickness $\delta = O(\nu x/U)^{\frac{1}{2}}$. If we are interested in situations where viscous and inertial effects are comparable for most of the flow domain, necessarily this must mean that the boundary layers fill most or all of the gap, i.e. that $\delta = O(h_0)$ when $x = O(L)$, which demands again that $R = O(1)$.

We can also see how the two limits $R \to 0$ and $R \to \infty$ operate to yield lubrication and aerodynamic flows respectively. If $R \to 0$, the effect (providing $p$ has the scale $p_V$) is that the inertia terms on the left of (1.9) become of vanishing importance, and hence $\psi$ is cubic in $y$. On the other hand, if $R \to \infty$, while $p$ has the scale $p_I$, the term $\nu \psi_{yyy}$ is negligible (except in boundary layers of vanishing thickness at $y = 0$ and $y = h(x)$), and inviscid-fluid theory applies almost everywhere.

What we have not yet incorporated is appropriate end conditions. This is not at all a straightforward matter, and the correct choice of end conditions in general depends on the nature of the flow *outside* the narrow-gap region. Hence, there may be many such types of end conditions. In the section that follows, we derive the appropriate end conditions for the sliding-sheet problem.

It is, however, clear that the usual $p = 0$ conditions are expected to hold in the lubrication limit $R \to 0$. That is, most external flows will *not* be viscosity-dominated to the extent that the gap-flow is so dominated at $R \to 0$, and hence the end conditions will tend to prescribe pressures at entrance and exit, that are of the order of $p_I$, rather than $p_V$. Thus, if $R \to 0$, irrespective of what $O(p_I)$ values are prescribed at $x = 0$ and $x = L$, these values will appear to be vanishingly small relative to $p_v$, and may be taken as zero, to leading order as $R \to 0$. Note that the above pressure argument makes no assumptions about the detailed nature of the inlet velocity profile, so long as it is such that $p = O(p_I)$.

What is more interesting and important is the conclusion that, as soon as we *do*

wish to take some account of inertia, we must *abandon* the $p = 0$ conditions. The lubrication-theory literature contains many examples where corrections to Reynolds' equation are made to take *some* account of inertia, but these are inconsistent, unless the end conditions are *simultaneously* corrected, i.e. unless the solution starts and ends correctly.

However, in view of the parabolic nature of (1.9), insofar as $\psi(x, y)$ and the resulting velocity field is concerned, we need only concern ourselves with *starting* the computation correctly. Indeed we *cannot* prescribe more than the starting velocity profile, via $\psi(0, y)$. However, since only the pressure *gradient* $p'(x)$ appears in (1.9), the absolute value of the pressure remains free as an additional input parameter.

At first sight this is hardly a significant observation, since in any case $p(x)$ is only meaningful relative to some external or ambient datum. However, what is really of significance is the *change* in pressure $p(L) - p(0)$ between exit and entrance. For example, if $p(L)$ is given an arbitrary value (say, zero), then $p(0)$ must be specified, by matching with some external flow. In fact, there is an essential coupling between this pressure end condition, and the entrance velocity profile, or at least with its net volumetric flow.

This is best illustrated by anticipating the results for the sliding-sheet example, to be discussed in §2, in which the end conditions are

$$\psi = u_0 y, \quad p = \tfrac{1}{2}\rho U^2 - \tfrac{1}{2}\rho u_0^2 \quad \text{at} \quad x = 0, \tag{1.12}$$

$$p = 0 \quad \text{at} \quad x = L, \tag{1.13}$$

where $u_0$ is a constant *to be determined*. That is, in this case the entrance flow is a uniform stream of *a priori unknown* magnitude $u_0$. The pressure at the entrance is set at the value predicted by Bernoulli's equation for that (indeterminate) flow, and must return to its (zero) ambient value at the exit $x = L$. The problem must be solved in an inverse manner, with $u_0$ varied until the solution satisfies (1.13).

We provide here a numerical solution of the problem so formulated. That is, we solve the boundary-layer equation (1.9), subject to (1.10) on $y = 0$ and (1.11) on $y = h(x)$, with (1.12) at $x = 0$ and (1.13) at $x = L$. Equivalent to (1.11) in these circumstances are

$$\psi = u_0 h_0, \quad \frac{\partial \psi}{\partial n} = 0 \quad \text{on} \quad y = h(x). \tag{1.14}$$

The problem is solved (*a*) by linearizing, and (*b*) by finite differences. Linearization is a well-accepted technique for this type of problem (cf. Sparrow *et al.* 1964) but is only empirically based. However, in the present case, it leads to a relatively simple explicit formula for $p(x)$, from which output quantities such as net lift force and centre of pressure location can be computed easily, with accuracies within about 10%.

Direct finite-difference solution is in principle capable of yielding arbitrarily accurate solutions of the problem, but at the cost of considerable computational effort. In the present paper, a simple unsophisticated algorithm is used to check the accuracy of the linearized formula, and to provide a limited amount of 'exact' output information for the sliding-sheet problem.

## 2. Matching for sliding thin bodies

Consider the flow sketched in figure 1. A thin airfoil-like body is located close to the plane $y = 0$, so that both its upper surface $y = h^+(x)$ and its lower surface $y = h(x)$ satisfy for $0 \leqslant x \leqslant L$,

$$h, h^+ = O(\epsilon) L, \tag{2.1}$$

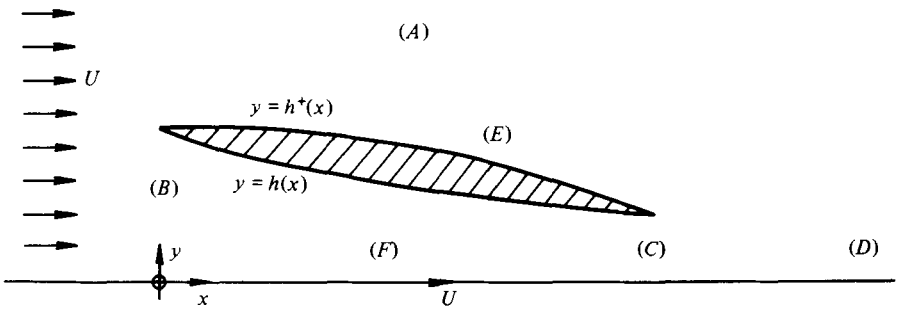


FIGURE 1. Sketch of flow situation for sliding sheets. The notation (*A*), (*B*), etc., denotes asymptotic regions defined in §2.

where $\epsilon$ is a small parameter and $L$ is the body's length. An incompressible Newtonian viscous fluid flows past this fixed body, in such a way that there is a uniform stream $U$ in the $x$-direction at infinity. In order that this flow at infinity be compatible with the existence of the plane non-slip boundary surface $y = 0$, we assume that this plane consists of a 'moving belt', which is itself moving at speed $U$ in the $+x$-direction. Thus this flow is identical to what would be seen by an observer moving at speed $U$ in the $-x$-direction, accompanying a moving airfoil in the presence of a fixed plane wall $y = 0$, in an otherwise stationary fluid.

In general, we must satisfy the Navier–Stokes equation

$$\psi_y \nabla^2 \psi_x - \psi_x \nabla^2 \psi_y = \nu \nabla^4 \psi \tag{2.2}$$

everywhere in the flow domain, subject to

$$\psi_x = \psi_y = 0 \quad \text{on} \quad y = h(x), h^+(x), \tag{2.3}$$

$$\psi_x = 0, \quad \psi_y = U \quad \text{on} \quad y = 0, \tag{2.4}$$

$$\psi \to Uy \quad \text{as} \quad y \to +\infty. \tag{2.5}$$

We see an asymptotic solution as $\epsilon \to 0$, for fixed $O(1)$ values of

$$R = \epsilon^2 UL/\nu. \tag{2.6}$$

If $h_0 = h(0) = O(\epsilon L)$ is a typical measure of the distance between wall and body, it is convenient to define also the Reynolds numbers based on $L$ and on $h_0$, i.e.

$$R_L = \frac{UL}{\nu} = \epsilon^{-2} R, \tag{2.7}$$

$$R_h = \frac{Uh_0}{\nu} = \epsilon^{-1} R, \tag{2.8}$$

noting that, if $R = O(1)$, both $R_L$ and $R_h$ are large.

As $\epsilon \to 0$, we need to solve by matching various regions of flow. These include:

(*A*) the outer region $x = O(L)$, $y = O(L)$;

(*B*) the entrance region $x = O(h_0)$, $y = O(h_0)$;

(*C*) the exit region $x = L + O(h_0)$, $y = O(h_0)$;

(*D*) the wake region $x = O(L) > L$, $y = O(h_0)$;

(*E*) the upper boundary-layer region $x = O(L)$, $y = h^+(x) + O(h_0)$;

(*F*) the gap region $x = O(L)$, $0 < x < L$, $0 < y < h(x)$;

as indicated in figure 1. In order to establish the correct equations to be satisfied in

these various regions, it is only necessary to perform the appropriate coordinate non-dimensionalization in each case. The $x$-wise velocity scale is taken as $U$ in all regions.

For example, in the outer region ($A$), both coordinates are scaled by $L$. Hence (2.2) simply scales to itself, with $\nu$ replaced by $1/R_L$. But, since $R_L = O(\epsilon^{-2}) \to \infty$ when $\epsilon \to 0$, this means that, to leading order, viscous forces can be neglected in the outer region. Since the flow is irrotational far upstream, Kelvin's circulation theorem demands that it is irrotational everywhere. Thus, we have to solve a classical-hydrodynamic problem for irrotational flow past a fixed surface. But, since that surface is a small $O(\epsilon)$ perturbation of the plane $y = 0$, the outer flow is therefore such a small perturbation of a uniform stream, and we may write

$$\psi = Uy + O(\epsilon) \tag{2.9}$$

throughout the outer region.

For the most part, we shall not need to concern ourselves with the $O(\epsilon)$ correction to the uniform stream. However, we shall at least need to observe that this correction can be written as a distribution of sources and sinks over the plane $y = 0$. If $x < 0$, the source strength is zero, since the only effective boundary is the undisturbed plane $y = 0$. If $x > 0$, the perturbation to the uniform stream is induced by an $O(\epsilon)$ perturbation, say $y = \bar{h}(x)$, in the boundary. If $0 < x < L$, $\bar{h}(x)$ consists of the original upper boundary $h^+(x)$, plus the thickness of the upper boundary layer. If $x > L$, $y = \bar{h}(x)$ is the equation of the wake boundary, which is a continuous extension across $x = L$ of the upper surface of this boundary layer. The surface $y = \bar{h}(x)$ thus appears like the upper boundary of a semi-infinite symmetrical airfoil, and thin-airfoil theory (Newman 1977, p. 129) tells us that it is generated by a source distribution of $O(\epsilon)$ strength $2U\bar{h}'(x)$ per unit length.

However, this body need not be 'closed'; there could be an apparent 'hole' at its nose. That is, in addition to the continuous distribution of sources in $x > 0$, we shall have to allow for the possibility of a discrete source or sink at $x = 0$, whose $O(\epsilon)$ flux $m$ is (for the moment) unknown. Although in principle a similar isolated source or sink could be present at $x = L$ also, we exclude this possibility, since it leads to solutions that cannot match the exit conditions. On the other hand, the leading-edge source $m$ is of very great significance, since it determines in what proportions fluid passes over and under the airfoil, and hence ultimately the circulation around it and the lifting forces on it.

Now, if we turn to the entrance and exit regions, in both cases the appropriate lengthscale is $h_0$, and hence the Navier–Stokes equation (2.2) again scales to itself, but now with $\nu$ replaced by $1/R_h$. But again, $R_h$ is large (though not as large as $R_L$), and hence, in the limit as $\epsilon \to 0$, viscous forces can be neglected in both entrance and exit regions.

In the entrance region ($B$), the flow must match an irrotational flow far upstream, and again Kelvin's theorem demands that it be irrotational everywhere. The only boundaries are the original wall $y = 0$, $-\infty < x < \infty$, and a semi-infinite plane wall $y = h_0$, $0 < x < \infty$. If $(r, \theta)$ are polar coordinates, the entrance flow, valid in $r = O(h_0)$ must match as $r/h_0 \to \infty$, the limit as $r/L \to 0$ of the outer-region flow. But, as we have seen, the latter is a combination of a uniform stream $U$ and a source of (unknown) $O(\epsilon)$ strength $m$. Thus the boundary condition on the entrance-flow stream function at infinity is

$$\psi \to Uy + \frac{m}{2\pi}(\theta - \pi) \quad \text{as} \quad r \to \infty. \tag{2.10}$$

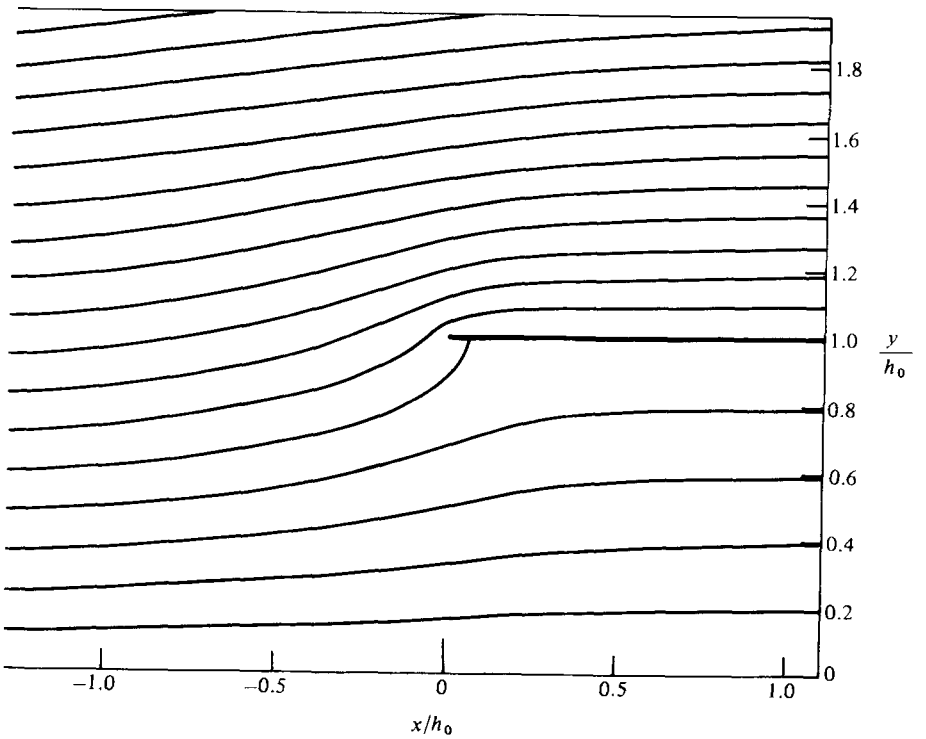


FIGURE 2. Streamlines for the irrotational entrance-region flow, computed from the exact conformal-mapping solution at $u_0/U = 0.5$ for equally spaced $\psi$-values.

This irrotational entrance flow can be determined completely by conformal-mapping methods. If $z = x + iy$ then the transformation

$$-\frac{\pi}{h_0} z = \zeta + \log \zeta + 1 \tag{2.11}$$

maps the flow region into the lower-half $\zeta$-plane. The solution for the complex potential $f = \phi + i\psi$ is then

$$-\frac{\pi}{h_0} f = U\zeta + u_0 \log \zeta, \tag{2.12}$$

where $u_0$ is a constant, related to $m$ by the equation

$$m = 2h_0(U - u_0). \tag{2.13}$$

It can readily be verified that, when $\zeta \to \infty$, we recover (2.10). On the other hand, if we let $\zeta \to 0$, we have $x/h_0 \to +\infty$ with $0 < y < h_0$, and in that limit

$$\psi \to u_0 y. \tag{2.14}$$

That is, as $x \to \infty$ underneath the airfoil (within its entrance region), we obtain a uniform stream of yet-to-be-determined magnitude $u_0$. All we know at the moment about $u_0$ is that its magnitude is of the same formal order with respect to $\epsilon$ as $U$, since (2.13) then allows $m = O(\epsilon)$, as required. If $u_0$ happens to equal $U$, then $m = 0$. This is the case when the airfoil traps exactly (and only) those streamlines that would have passed beneath it if it had presented no obstacle at all to the stream. If $u_0 < U$, then $m > 0$, and some streamlines are diverted over the top.

Figure 2 shows streamlines computed from (2.11) and (2.12) for $u_0/U = 0.5$. There

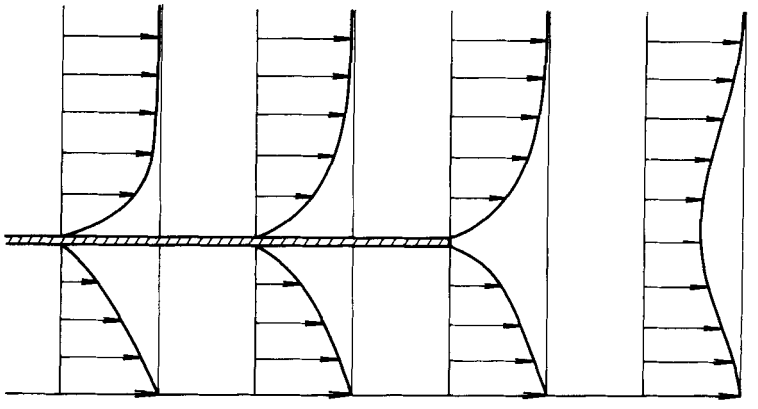

FIGURE 3. Sketch of possible exit-region velocity profiles.

is a stagnation point on the lower surface of the airfoil, just downstream of the leading edge. These streamlines are equally spaced in $\psi$ values, and the one-half speed reduction under the airfoil is displayed in a doubling in the asymptotic $y$-wise spacing there.

Associated with the irrotational flow in the entrance and outer regions is a pressure distribution, obtainable from Bernoulli's equation. Thus, if the ambient pressure at infinity is taken as zero, we have

$$\frac{p}{\rho} + \tfrac{1}{2}q^2 = \tfrac{1}{2}U^2, \tag{2.15}$$

where $q$ is the velocity magnitude. We shall only be interested in the limit of (2.15) when $x$ is large compared with $h_0$, within the entrance region and under the airfoil, namely (from (2.14)),

$$p \to \tfrac{1}{2}\rho(U^2 - u_0^2). \tag{2.16}$$

That is, the pressure 'far' to the right (in the gap) of the entrance is related quadratically to the (as yet unknown) uniform velocity $u_0$ across the gap at that station. The behaviour (2.13) of the stream function, and (2.16) of the pressure, must now match with the *initial* behaviour of the gap-region flow at $x/L = 0$.

Turning now to the *exit* region ($C$), although it is still true that viscous forces are negligible, we can no longer call upon Kelvin's theorem to prove irrotationality, since the gap flow upstream of the exit is rotational. Indeed, there is bound to be considerable vorticity in the exit region, and in the wake region that follows it. Figure 3 sketches the type of velocity profiles that might be expected during the 'gap–exit–wake' transition. However, as with the outer region, we are not really interested in all of the details of the flow in this region. In fact, we have no other use for this region than to observe that $p = O(\epsilon)\rho U^2$ throughout it.

This important conclusion follows from the fact that $p = O(\epsilon)\rho U^2$ everywhere in the outer region also, by (2.15) and (2.9). But the exit region simply provides a smooth merging of various boundary layers. As with any boundary layer, the change in pressure across the layer is of a relative amount at most $O(\epsilon^2)$, and hence the pressure in the exit region is also $O(\epsilon)\rho U^2$.

It is of value to contrast the exit and entrance regions, with respect to pressure orders. The entrance pressure is *not* small, only because of the source $m$. If $m \neq 0$,

then $u_0 \neq U$, and $p$ in (2.16) is of the order of $\rho U^2$. But we do not allow an equivalent to the source $m$ at the exit region, and hence $p$ is always small there. The conclusion that $p = O(\epsilon)\rho U^2$ in the exit region means that, relative to the $O(\rho U^2)$ values now of interest in the gap, the gap flow must match the exit flow at $x = L$ with *zero* pressure.

In the wake ($D$), and gap ($F$) regions, the $x$-scale is $L$ and the $y$-scale is $h_0 \ll L$. Hence, no longer does the Navier–Stokes equation (2.2) scale into itself. In effect, we can neglect the operator $\partial/\partial x$ relative to $\partial/\partial y$ in the limit as $\epsilon \to 0$, and (2.2) simplifies to

$$\psi_y \psi_{xyy} - \psi_x \psi_{yyy} = \nu \psi_{yyyy}. \tag{2.17}$$

If actual scaled coordinates are employed, $\nu$ in (2.17) is replaced by $1/R$, where $R$ is defined by (2.6). Thus, when $R = O(1)$ (as we are assuming), viscous effects are felt only in these regions. Equation (2.17) is also known to hold in the upper boundary layer ($E$).

However, in the present context, we have very little interest in the wake or in the upper boundary layer, since in neither of these two regions does the pressure depart significantly from the free-stream (zero) value. As shown by Bentwich (1978), the wake is a region in which the fluid velocity is returning rapidly to the value $U$ enforced by the moving plane $y = 0$, and the detailed manner of approach to a uniform flow can easily be computed by linearizing about it. The upper boundary layer is to leading order of a conventional Blasius character, and has a negligible effect on the flow in the gap region.

Finally, we come to the all-important gap region. In fact, all other regions serve only to determine the initial and final conditions for the gap-region flow, and, having done so, can be ignored henceforth.

Our task is thus to solve (2.17), subject to 4 boundary conditions, namely (2.3) on the *lower* surface $y = h(x)$ only, and (2.4) on $y = 0$. We also need an initial condition on $\psi$ at $x = 0$. But this is just (2.14), i.e. the assertion that the flow at the start of the gap matches the uniform stream $u_0$ at the right edge of the entrance region. Since $u_0$ is still an unknown constant, (2.14) at first sight hardly appears to serve the purpose of an initial condition. However, if we integrate (2.17) once with respect to $y$, yielding the usual boundary-layer equation (1.9), and introducing thereby the pressure gradient $p'(x)$, we close the loop by also demanding that the pressure start with the value (2.16) at $x = 0$, and end with a zero value at $x = L$. Equivalently, the pressure *gradient* must satisfy

$$\int_0^L p'(x)\,\mathrm{d}x = -\tfrac{1}{2}\rho(U^2 - u_0^2). \tag{2.18}$$

Equation (2.18) can be thought of as a 'normalization' condition, that ultimately determines the parameter $u_0$.

## 3. Linearized solution

Suppose that $\overline{U}(x)$ is some measure of the mean $x$-wise velocity $\psi_y$, averaged across the gap with respect to $y$, at fixed station $x$. Then, as an empirical approximation, we suppose that the nonlinear convection terms on the left of (1.9) can be estimated by linearizing about $\overline{U}(x)$. That is, we write formally

$$\psi(x, y) = \overline{U}(x)\, y + \psi_1(x, y) \tag{3.1}$$

and neglect all terms that are quadratic in $\psi_1$, obtaining

$$\bar{U}(x)\,\psi_{xy} - \bar{U}'(x)\,[y\psi_{yy} - \psi_y + \bar{U}(x)] = -\frac{1}{\rho}p'(x) + \nu\psi_{yyy}, \tag{3.2}$$

which is a linear equation for $\psi$.

Note that replacement of (1.9) by (3.2) is consistent with lubrication theory in the limit as $R \to 0$ (since in any case the whole left-hand side is neglected in that limit), and also with inviscid small-gap theory in the limit as $R \to \infty$ (since that theory has the property that $\psi \equiv \bar{U}y$). For intermediate $R$-values, it is not entirely clear *a priori* how good an approximation (3.2) is. However, similar approximations (cf. Sparrow *et al.* 1964) have become standard in entrance-flow calculations.

Although (3.2) is linear, it is still not straightforward to solve, for general $\bar{U}(x)$. However, in the special case where

$$\bar{U}(x) = U_0 h_0 / h(x) \tag{3.3}$$

for some constant $U_0$, a further simplification occurs, and a closed-form solution can be found. Note that the inviscid small-gap solution has the property (3.3), with $U_0 = u_0$, and we expect that $U_0 \simeq u_0$ in general, since that choice means that the net flux of $\bar{U}(x)$ agrees with that for the actual solution $\psi$.

Suppose we substitute

$$\psi = \frac{U_0 h^2}{h_0}\phi(X, Y), \tag{3.4}$$

where

$$X = \frac{\nu}{U_0 h_0}\int_0^x \frac{\mathrm{d}x}{h(x)}, \tag{3.5}$$

$$Y = y/h(x). \tag{3.6}$$

Then (3.2) becomes

$$\phi_{YYY} - \phi_{XY} = P'(X), \tag{3.7}$$

where

$$P(X) = \frac{p}{\rho U_0^2} - \frac{1}{2}\frac{h_0^2}{h^2}. \tag{3.8}$$

Equation (3.7) can be differentiated once with respect to $Y$ to eliminate the pressure term; thus we have finally a very simple partial differential equation

$$\phi_{YYYY} = \phi_{XYY} \tag{3.9}$$

whose solution can be obtained by various standard methods. Note that (3.9) is a diffusion equation for the shear $\phi_{YY}$.

It is convenient to restrict attention to the case of a flat plate at angle of attack $\alpha$, i.e. to assume that $h(x)$ is given by (1.2). Then, from (3.5)

$$h/h_0 = \mathrm{e}^{-\beta X}, \tag{3.10}$$

where

$$\beta = U_0 h_0 \alpha / \nu. \tag{3.11}$$

If we define the Laplace transform

$$\bar{\phi}(s, Y) = \int_0^\infty \phi(X, Y)\,\mathrm{e}^{-sX}\,\mathrm{d}X, \tag{3.12}$$

it can then be shown that (with $t = s^{\frac{1}{2}}$),

$$U_0\bar{\phi}(s, Y) = \frac{UY}{s-\beta} + \frac{\cosh(tY)-1}{\Delta}\left[U\frac{\sinh t - t\cosh t}{t(s-\beta)} + u_0\frac{\cosh t - 1}{s-2\beta}\right] + \frac{\sinh(tY)-tY}{\Delta}\left[U\frac{t\sinh t - \cosh t + 1}{t(s-\beta)} - u_0\frac{\sinh t}{s-2\beta}\right] \quad (3.13)$$

satisfies all requirements, if

$$\Delta(s) = 2 - 2\cosh t + t\sinh t. \quad (3.14)$$

That is, (3.13) clearly is a solution of the equation resulting from Laplace transforming (3.9), vanishes on $Y = 0$, and $\bar{\phi}_Y(s, 0)$ is the Laplace transform of

$$\phi_Y(X, 0) = \frac{U}{U_0}\frac{h_0}{h}, \quad (3.15)$$

as required by (1.10), (3.4) and (3.6). Similarly, $\bar{\phi}_Y$ vanishes at $Y = 1$, and $\bar{\phi}(s, 1)$ is the Laplace transform of

$$\phi(X, 1) = \frac{u_0}{U_0}\frac{h_0^2}{h^2}, \quad (3.16)$$

as required by (1.14) and (3.4). The initial condition (1.12) is satisfied, as can be verified by letting $s \to \infty$ in (3.13).

The corresponding pressure can be evaluated from (3.7) and (3.8). Thus from (3.7)

$$U_0\bar{P}(s) = \frac{U_0 P(0) + u_0}{s} - \frac{U}{s-\beta} + \frac{1}{\Delta}\left[U\frac{t\sinh t - \cosh t + 1}{s-\beta} - \frac{u_0 t\sinh t}{s-2\beta}\right]. \quad (3.17)$$

Hence from (3.8), using (1.12) for $p$ at $x = 0$,

$$\frac{\bar{p}(s)}{\rho} = \frac{U^2 - (u_0 - U_0)^2}{2s} - \frac{U_0 U}{s-\beta} + \frac{1}{2}\frac{U_0^2}{s-2\beta} + \frac{U_0}{\Delta}\left[U\frac{t\sinh t - \cosh t + 1}{s-\beta} - \frac{u_0 t\sinh t}{s-2\beta}\right]. \quad (3.18)$$

In order to take the inverse transform of (3.18), we need merely observe that $\bar{p}(s)$ is singular *only* where $s = 0, \beta, 2\beta$, and at zeros of $\Delta(s)$. All such singularities can be shown to be simple poles, whose residues can be evaluated. Thus, we can write as our final solution for the pressure

$$\frac{p(x)}{\rho} = \tfrac{1}{2}U^2 - \tfrac{1}{2}(u_0 - U_0)^2 + 6U_0(u_0 - U) - U_0 U\left[1 - \frac{\beta^{\frac{1}{2}}\sinh\beta^{\frac{1}{2}} - \cosh\beta^{\frac{1}{2}} + 1}{\Delta(\beta)}\right]\frac{h_0}{h(x)} + U_0\left[\frac{U_0}{2} - \frac{u_0(2\beta)^{\frac{1}{2}}\sinh(2\beta)^{\frac{1}{2}}}{\Delta(2\beta)}\right]\left(\frac{h_0}{h(x)}\right)^2 - 4U_0\sum_{m=1}^{\infty}\left[\frac{U}{k_m^2+\beta} - \frac{2u_0}{k_m^2+2\beta}\right]\left(\frac{h(x)}{h_0}\right)^{k_m^2/\beta}, \quad (3.19)$$

where $z = \frac{1}{2}k_m$ is the $m$th root of the transcendental equation

$$\tan z = z. \quad (3.20)$$

Note that $s = -k_m^2$ is a zero of $\Delta(s)$; there are also zeros of $\Delta(s)$ at $s = -4m^2\pi^2$, which contribute to $\phi$ but not to $p$. In practice, since the lowest value of $k_m^2$ is about 80, the sum in (3.19) is negligible for most $x > 0$, unless $\beta$ is quite large. The series converges at $x = 0$, when $h(x)/h_0 = 1$, because $k_m \to (m + \frac{1}{2})\pi$ as $m \to \infty$. However, its derivative with respect to $x$ then does *not* converge at $x = 0$. That is, the initial pressure gradient is infinite. Indeed, it is a well-known property of such series that

$p'(x)$ possesses an inverse-square-root singularity as $x \downarrow 0$;† this property also follows from (3.17) as $s \to \infty$, and is discussed further in §5.

We can use (3.19) directly to solve the actual sliding-sheet problem, as follows. First we set $x = L$, i.e. $h(x)/h_0 = 1 - \alpha L/h_0$, and evaluate $p(L)$ for a range of values of $u_0$. We then select $u_0$ (by trial and error, although an automatic search could have been implemented) so that $p(L) = 0$. The net lift force

$$F = \int_0^L p(x)\,\mathrm{d}x \tag{3.21}$$

and moment

$$M = \int_0^L xp(x)\,\mathrm{d}x = Fx_\mathrm{p}, \tag{3.22}$$

where $x = x_\mathrm{p}$ is the location of the centre of pressure, are then computed by evaluating $p(x)$ at that value of $u_0$, and using Simpson's rule.

The arbitrary linearization parameter $U_0$ is generally set equal to $u_0$. Numerical experimentation revealed that very wide variations, e.g. $U_0/u_0$ values ranging from 0.5 to 2.0, changed the value of $F$ by less than 2%, and had almost no effect at all on $x_\mathrm{p}$. This is a satisfactory conclusion, since insensitivity to the actual value of $U_0$, confirms that the linearization process is acceptable. So long as convection is allowed to take place, it is not of major significance to convect at exactly the right speed everywhere.

## 4. Numerical boundary-layer solution

The linearized solution (3.19) is explicit, and reasonably simple to use. However, it is based on an ad hoc linearization of the true governing boundary-layer equation (1.9). Clearly, a more satisfactory procedure would be to solve (1.9), or equivalently (2.17), by direct numerical methods. There are many such methods in the literature, e.g. as surveyed by Blottner (1975) or Keller (1978).

In spite of its parabolic character, which means that solution can proceed by 'marching' forward in the $x$-direction, at considerable saving over the elliptic Navier–Stokes equation (2.2), the boundary-layer equation (2.17) still presents formidable computational difficulties. In the present problem, remembering that solutions have to be repeated for a range of values of $u_0$ at every separate specified Reynolds number and angle of attack, it is perhaps not reasonable to expect that such solutions can be used routinely. Instead, our present aim is to provide a few 'benchmark' numerical solutions, of effectively unlimited accuracy, to test the validity of the linearized solution (3.19).

For that purpose, we have implemented the following relatively crude, but systematically improvable, algorithm. We use simple first-order-accurate backward differences with $x$-wise spacing $\Delta x$, i.e. set

$$\psi_x(x, y) \simeq \frac{\psi(x, y) - \psi(x - \Delta x, y)}{\Delta x}, \tag{4.1}$$

for all $x > \Delta x$. At the first non-zero station $x = \Delta x$, we *halve* (4.1), in order to model an $x^{\frac{1}{2}}$ initial dependence on the $x$-variable. The accuracy of the final results is a function of the spacing $\Delta x$, which can be reduced until an acceptable degree of precision is attained.

† We are indebted to Dr Jane Pitman for this observation.

If (4.1) is used to estimate $\psi_x$ and $\psi_{xyy}$ in (2.17), with $\psi$ and $\psi_{yy}$ assumed known at the previous station $x-\Delta x$, then (2.17) becomes a 4th-order nonlinear ordinary differential equation, for $\psi(x, y)$ as a function of $y$, at fixed $x$. This ordinary differential equation can, in principle, be solved to arbitrary precision. In practice, we use a finite grid of $N$ points between $y = 0$ and $y = h(x)$, and systematically increase $N$ until the solution has converged to within acceptable accuracy. The actual 4th-order problem is a 2-point boundary-value problem, with $\psi, \psi_y$ values prescribed at $y = 0$ and $y = h(x)$. Naive 'shooting' methods, in which Runge–Kutta initial-value solutions are Newton-iterated with respect to $\psi_{yy}, \psi_{yyy}$ values at $y = 0$, until the solution fits the required $\psi, \psi_y$ values at $y = h(x)$, seem to work quite adequately.

Results with 2–3-figure accuracy were obtainable using $N = 20$ points in the $y$-direction, although up to $N = 50$ was used for verification. As far as the $x$-wise spacing is concerned, $\Delta x/L = 0.05$ was adequate except near $x = 0$, and $\Delta x/L = 0.01$ was sometimes needed up to $x/L = 0.1$. It is also only for small $x$ that large $N$-values are ever required, since only then are there rapid variations with respect to $y$, in the boundary layers near the walls.

The pressure gradient is a direct output, being proportional to the quantity $\psi_{yyy}(x, 0)$ that is used as an iteration parameter to solve the 2-point boundary-value problem. The pressure itself is obtained by trapezoidal integration, with a leading-edge correction for the $x^{\frac{1}{2}}$ behaviour, and subject to the initial value given by (1.12).

As inputs, we need the Reynolds number $R$ and angle of attack $\alpha$. We must then select a value of $u_0$ and make a run from $x = 0$ to $x = L$. If $p = 0$ at that point, we are successful; otherwise we try a different $u_0$. An initial choice for $u_0$ is obtained from the linearized solution, and in principle we must then repeat the solution for a range of $u_0$ values, and select one such that the desired exit condition is satisfied. However, the linearized theory appears to be very accurate (within 1 %) as a prediction of the correct $u_0$ value, so that very little such adjustment is needed. An additional feature reducing computational effort, is that one can re-scale the problem. That is, should $p = 0$ at a value $L_1 \neq L$, the solution so obtained can be re-interpreted as that for a new Reynolds' number $R_1 = RL/L_1$.

Converged results for the pressure, and its integrals for the lift and centre of pressure, with accuracies better than 0.5 %, were obtained for 6 combinations of Reynolds number and angle of attack, and these are discussed in §5.

## 5. Discussion of results

Results have been obtained using the numerical method described above, for various values of $R$ and of the scaled angle of attack

$$\bar{\alpha} = \frac{\alpha L}{h_0} = 1 - \frac{h(L)}{h(0)}, \tag{5.1}$$

which also measures the contraction rate of the converging channel. For the most part we concentrate on the pressure distribution $p(x)$.

However, information about the actual fluid velocity is available and of interest, and figure 4 shows a set of computed streamlines for $R = 9.6$, $\bar{\alpha} = 0.75$. Note that the vertical scale is $h_0$, and the horizontal scale is $L$; thus all streamlines in fact make small angles to the horizontal, as required, when $h_0 \ll L$. The streamlines shown are not claimed to be of high accuracy, since they were obtained by interpolating roughly, from $N = 20$ output $\psi$ values.

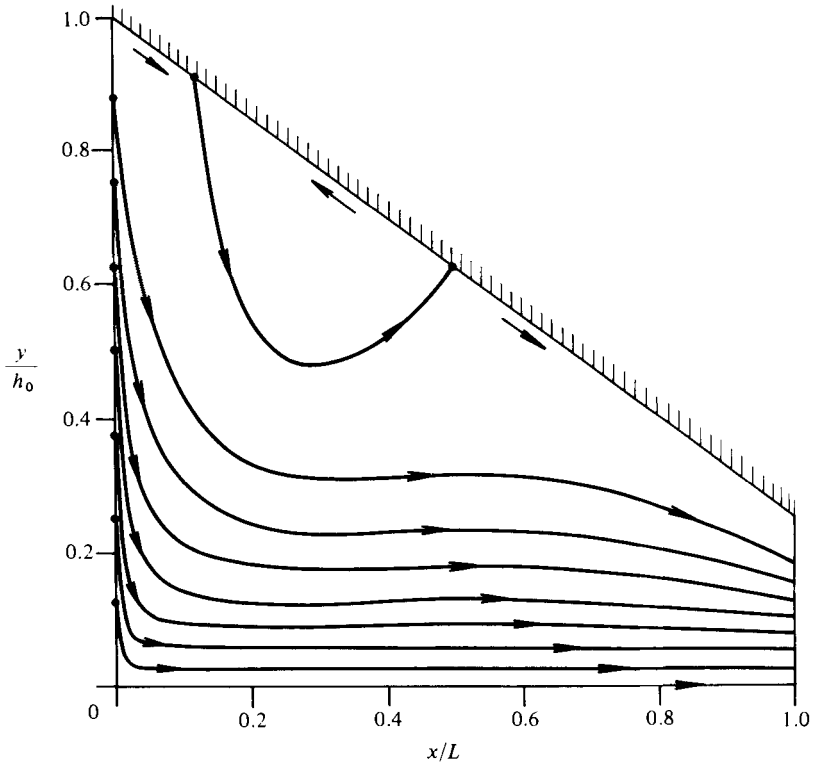


FIGURE 4. Streamlines of gap-region flow at $R = 9.6$, $\bar{\alpha} = 0.75$.

The most interesting feature of figure 4 is a recirculating 'bubble' attached to the upper boundary, with reversed flow near that boundary. The wall shear $\psi_{yy}$ vanishes at two points on that boundary.

Although this result is at first sight somewhat unexpected, it is one that also occurs within the context of lubrication theory (Schlichting 1960, p. 98). It can easily be shown (cf. Michell 1950, p. 85) that, if $\bar{\alpha} > 0.5$, i.e. if the contraction rate of the converging channel is more than 2:1, reversed flow must occur near the beginning of the upper boundary, according to lubrication theory. However, in that case, there can be only one point on the wall where the shear $\psi_{yy}$ vanishes, i.e. lubrication theory demands that the flow already *commences* at $x = 0$ with a reversed flow near $y = h_0$. Now that we have incorporated inertia, and, more important, have *demanded* that the flow commence with a forward-flowing uniform profile at $x = 0$, the same reversed-flow phenomenon can still occur at subsequent stations $x > 0$, but must commence with one zero-shear point, and end with another.

Figures 5 and 6 give results for the pressure $p(x)$, for two cases $R = 0.6$, $\bar{\alpha} = 0.4$, and $R = 9.6$, $\bar{\alpha} = 0.75$ respectively. These are similar to the results obtained for other $R, \bar{\alpha}$ values, but represent the lowest and highest Reynolds numbers tried. In each case, we show:

(i) converged numerical boundary-layer solutions;

(ii) the linearized solution (3.19);

(iii) lubrication theory (1.3);

(iv) inviscid small-gap theory (1.4).

The computations of figure 5 are for a relatively low Reynolds number $R = 0.6$,

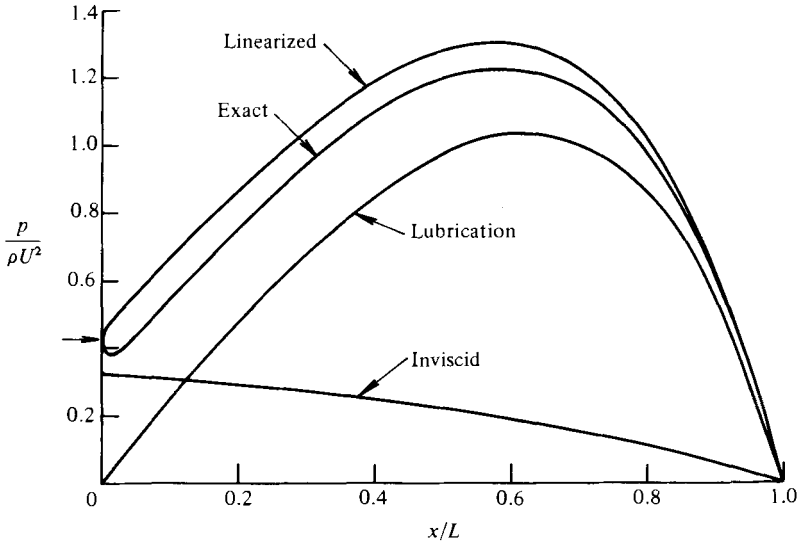


FIGURE 5. Pressure results at $R = 0.6$, $\bar{\alpha} = 0.4$.

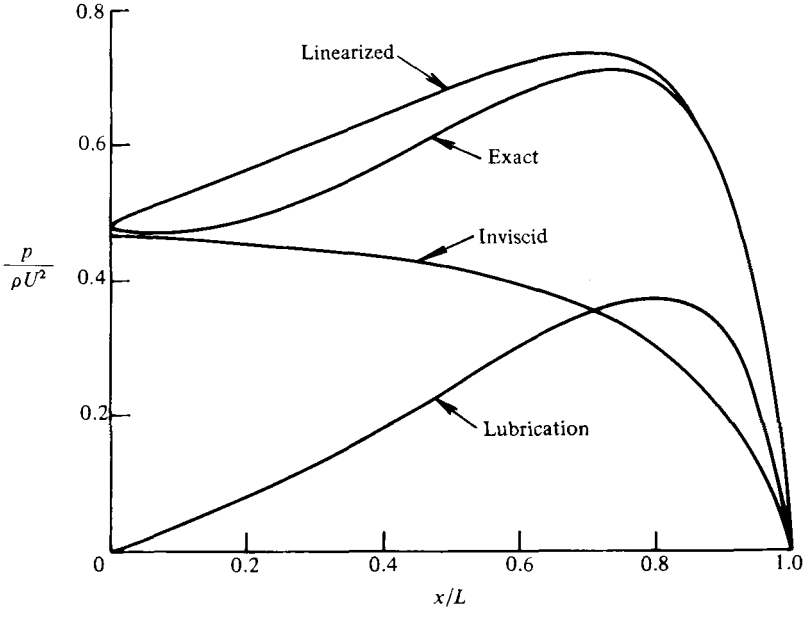


FIGURE 6. Pressure results at $R = 9.6$, $\bar{\alpha} = 0.75$.

at which we might expect lubrication theory to be reasonably accurate. This is true, in that the correct peak pressure is approximated to within 20% by lubrication theory. The main source of discrepancy is the difference in inlet condition. In the present finite-$R$ theory, the inlet velocity distribution is uniform, whereas lubrication theory assumes a parabolic distribution everywhere, including at the inlet. Of course *neither* assumption is strictly correct as a formal limiting result as $R \to 0$, and, for a correct low-Reynolds-number asymptotic theory near the inlet, we should have to revert to an elliptic Stokes-flow problem in which the flow just upstream of the inlet is affected by that in the gap (and vice versa).

Although, at such a low Reynolds number, we could not expect the inviscid theory to be valid, and this is confirmed by figure 5, an interesting phenomenon occurs at the very start of the gap, i.e. for small $x$. It is clear then that what happens at first is that boundary layers, of thickness $\delta = O(\nu x/u_0)^{\frac{1}{2}}$, start to grow at $x = 0$ on both walls $y = 0$ and $y = h_0$. The layer on the fixed wall $y = h_0$ is of conventional Blasius character, involving a change from a zero velocity at $y = h_0$ to the velocity $u_0$ as $(h_0 - y)/\delta \to \infty$. The layer on the moving wall $y = 0$ is also of a Blasius-similarity character, but is somewhat unconventional, in that it involves an adjustment between the wall velocity $U$ at $y = 0$ and $u_0$ as $y/\delta \to \infty$. In any case, it is clear that the initial effect is an $O(x^{\frac{1}{2}})$ shrinking of the effective gap width. Initially, this is of greater significance than the $O(x)$ convergence of the channel walls.

Meanwhile, an almost-uniform core flow takes place everywhere between these 2 thin boundary layers, whose magnitude starts out at $u_0$, but quickly changes. Indeed, this core flow is *correctly* described (at least in the limit of small $x$) by inviscid small-gap theory, and that theory predicts that its velocity must *increase* like $x^{\frac{1}{2}}$ to conserve mass, against the boundary-layer-induced narrowing of the gap. But this then implies that the core pressure *decreases* like $x^{\frac{1}{2}}$ initially; that is, the pressure gradient has a *negative inverse-square-root* singularity at $x = 0$. Note that this singularity is not strong enough to influence the initial development of the wall boundary layers, which remain (to leading order) of Blasius or zero-pressure-gradient similarity character.

The computed results confirm this initial behaviour in the pressure. The lower the Reynolds number $R$, the more closely confined to $x = 0$ does it occur, and eventually this presents formidable starting difficulties to the numerical analysis. However, $R = 0.6$ is not too low to enable converged results that display the behaviour. The scaled pressure in figure 5 drops quickly from its starting value 0.43, to a minimum of 0.38 at about $x = 0.015$, before increasing again, as the boundary layers absorb the core, and the effects of the converging walls begin to be felt.

Another remarkable feature of these results is that, once this increase occurs, the pressure then follows a curve that, if extrapolated backwards to $x = 0$, appears to emanate from the same value ($p = 0.32$ on figure 5) at which the *inviscid* theory commences. Note that this inviscid value corresponds to a different $u_0$ value, namely

$$u_0 = Uh(L)/h(0), \tag{5.2}$$

from that found as part of the 'exact' numerical solution.

By contrast to figure 5, figure 6 involves a relatively high Reynolds number $R = 9.6$. At the high-$R$ end of the range, numerical difficulties occur not only for small $x$, but (in principle) throughout the computation. In compensation, the square-root singularity at $x = 0$ is weaker, since the initial wall boundary layers stay thin longer. Thus inviscid small-gap theory retains validity over a range of early $x$ values, and that range increases as $R$ increases. At $R = 9.6$, this range still only amounts to about the first quarter of the gap length, and the inviscid theory fails to predict the peak pressure by a factor of 2. Thus for accurate inviscid results we should need to go to considerably higher $R$ still. Lubrication theory is of course already quite inaccurate at $R = 9.6$. It may or may not be a coincidence that, in both figures 5 and 6, if one *adds* the inviscid and lubrication results, one obtains a quite good approximation to the true pressure distribution.

The linearized computations also shown in figures 5 and 6 are very interesting. Generally, the linearized theory overestimates the pressure in the forward half of the gap by about 12%, but becomes accurate toward the trailing edge. The linearized theory, like the exact theory, possesses an inverse-square-root singularity in the

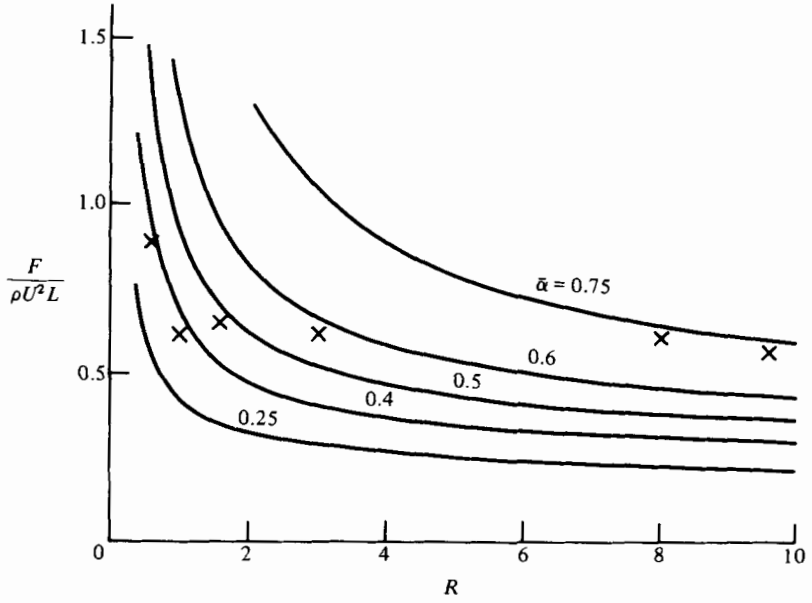


FIGURE 7. Net lift force as a function of Reynolds number $R$ for various contraction ratios $\bar{\alpha}$.

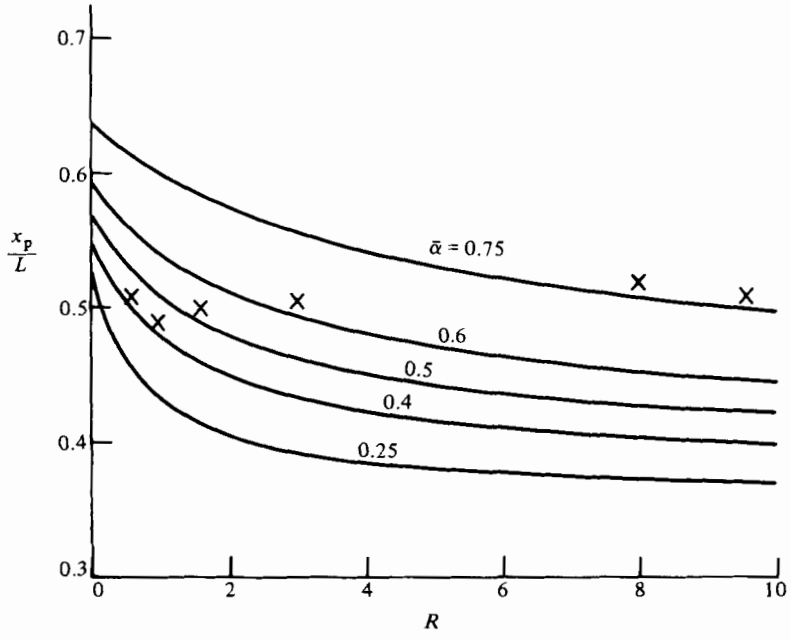


FIGURE 8. Location $x = x_p$ of centre of pressure as a function of Reynolds number $R$ for various contraction ratios $\bar{\alpha}$.

pressure gradient at $x = 0$ but this singularity is of the *wrong sign*, at least for $u_0/U < 0.5$. That is, according to the linearized theory, the pressure initially *increases* above its starting value, rather than decreases as it should.

In view of the fact that the process of linearization has destroyed any possibility of achieving nonlinear Blasius-type wall boundary layers, we should not be surprised

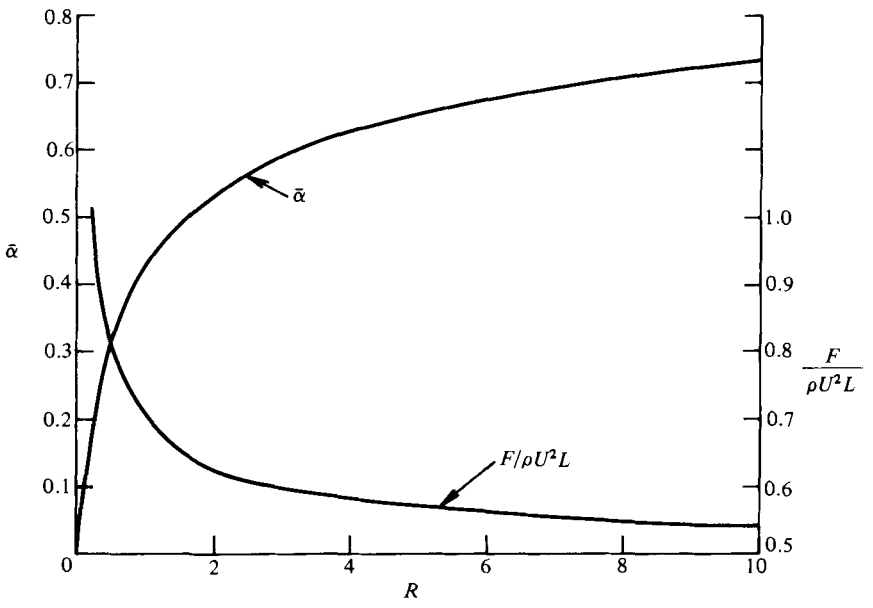


FIGURE 9. Net lift and contraction ratio as a function of Reynolds number $R$ for those solutions having $x_p/L = 0.5$.

that it fails to predict the initial pressure variation correctly. However, this does not seem to be a particularly serious defect from the arithmetical point of view, since, in spite of the incorrect sign to the pressure *gradient*, the pressure itself stays reasonably close to the correct value.

Figures 7 and 8 give results for the net lift force $F$ and centre of pressure $x_p$, as defined by (3.21) and (3.22) respectively. These are expressed as functions of Reynolds number $R$, for various values of $\bar{\alpha}$. The *curves* shown are based on the linearized theory. The 6 crosses represent 'exact' numerical boundary-layer solutions. Over the broad range of $R$, $\bar{\alpha}$ values shown, the linearized theory appears to *over*estimate $F$ by a consistent 10%, while *under*estimating $x_p$ by 5%. Lubrication theory can be used to give the asymptotic behaviour as $R \to 0$, and inviscid small gap theory as $R \to \infty$, in figures 7 and 8.

Finally, figure 9 gives plots of $F$ and $\bar{\alpha}$ against $R$, for those solutions such that $x_p = \frac{1}{2}L$. These results were obtained by extracting linearized values from figures 7 and 8, and applying the appropriate 10% and 5% corrections respectively. Figure 9 contains information that can be used to study the dynamics of freely sliding uniformly weighted sheets, whose total weight must equal $F$, and whose centre of gravity is located at $x = \frac{1}{2}L$.

## REFERENCES

BENTWICH, M. 1978 Semi-bounded slow viscous flow past a cylinder. *Q. J. Mech. Appl. Maths* **31**, 445–459.

BLOTTNER, F. G. 1975 *AGARD Lecture Series* no. 73, pp. 3.1–3.51.

CAMERON, A. 1966 *Principles of Lubrication*. Longmans.

KELLER, H. B. 1975 Some computational problems in boundary-layer flows. In *Proc. 4th Intl Conf. Numer. Meth. Fluid Dyn.* (ed. R. D. Richtmyer). Lecture Notes in Physics, vol. 35, pp. 1–21. Springer.

KELLER, H. B. 1978 Numerical methods in boundary layer theory. *Ann. Rev. Fluid Mech.* **10**, 417–433.

MICHELL, A. G. M. 1950 *Lubrication.* Blackie.

NEWMAN, J. N. 1977 *Marine Hydrodynamics.* M.I.T. Press.

SCHLICHTING, H. 1960 *Boundary Layer Theory*, 4th edn. McGraw-Hill.

SPARROW, E. M., LIN, S. H. & LUNDGREN, T. S. 1964 Flow development in the hydrodynamic entrance region of tubes and ducts. *Phys. Fluids* **7**, 338–347.

TUCK, E. O. 1980 A nonlinear unsteady one-dimensional theory for wings in extreme ground effect. *J. Fluid Mech.* **98**, 33–47.

TUCK, E. O. 1981 Steady flow and static stability of airfoils in extreme ground effect. *J. Engng Maths* **15**, 89–102.

TUCK, E. O. 1982 An inviscid theory for sliding flexible sheets. *J. Austral. Math. Soc.* (Ser. B) **23**, 403–415.

WILLIAMS, J. C. 1963 Viscous compressible and incompressible flow in slender channels. *AIAA J.* **1**, 186–195.